Published in final edited form as:
Neuron. 2011 December 8; 72(5): 819–831. doi:10.1016/j.neuron.2011.09.008.

Parallel regulation of feedforward inhibition and excitation during whisker map plasticity

David RC House[1,2], **Justin Elstrott**[2], **Eileen Koh**[2], **Jason Chung**[2], and **Daniel E. Feldman**[2,†]

[1]Neuroscience Ph.D. Program, University of California, San Diego, La Jolla, CA 92093

[2]Dept. of Molecular and Cellular Biology and Helen Wills Neuroscience Institute, University of California Berkeley, 142 LSA #3200, Berkeley, CA 94720

Abstract

Sensory experience drives robust plasticity of sensory maps in cerebral cortex, but the role of inhibitory circuits in this process is not fully understood. We show that classical deprivation-induced whisker map plasticity in layer 2/3 (L2/3) of rat somatosensory (S1) cortex involves robust weakening of L4-L2/3 feedforward inhibition. This weakening was caused by reduced L4 excitation onto L2/3 fast-spiking (FS) interneurons, which mediate sensitive feedforward inhibition, and was partially offset by strengthening of unitary FS to L2/3 pyramidal cell synapses. Weakening of feedforward inhibition paralleled the known weakening of feedforward excitation, so that mean excitatory-inhibitory balance and timing onto L2/3 pyramidal cells were preserved. Thus, reduced feedforward inhibition is a covert compensatory process that can maintain excitatory-inhibitory balance during classical deprivation-induced Hebbian map plasticity.

Keywords

vibrissa; somatosensory cortex; homeostatic plasticity; interneuron; fast-spiking; balance

Sensory experience shapes cortical sensory representations and perception. In classical sensory map plasticity, deprived sensory inputs weaken and shrink within maps, while spared or overused inputs strengthen and expand (Feldman and Brecht, 2005). This process involves multiple sites of plasticity in excitatory circuits, but how experience regulates inhibitory circuits is less clear, and may be more varied. In some cases, deprivation potentiates inhibition, which may suppress responses to deprived sensory inputs (Maffei et al., 2006). In other cases, deprivation weakens inhibition, which may homeostatically restore sensory responsiveness (Gandhi et al., 2008; Jiao et al., 2006; Maffei et al., 2004). A key factor is how deprivation affects excitation-inhibition balance, which is a major regulator of sensory tuning and information processing (Pouille et al., 2009; Wehr and Zador, 2003; Wilent and Contreras, 2005). Previous studies showed that deprivation can increase or decrease excitation-inhibition balance (Maffei et al., 2004; 2006; 2008; 2010). However, it may be essential to have a mode of cortical map plasticity that preserves normal excitation-inhibition balance, so that sensory processing is unimpaired in the reorganized map.

†Corresponding author. Correspondence should be addressed to: 142 Life Sciences Addition, Mail Code 3200, Dept. of Molecular and Cell Biology, Univ. of California, Berkeley, Berkeley, CA 92093-3200, dfeldman@berkeley.edu.

We studied how experience regulates feedforward inhibitory circuits and excitation-inhibition balance during whisker map plasticity in layer 2/3 (L2/3) of rodent somatosensory (S1 or barrel) cortex. L2/3 is the primary site of plasticity in post-neonatal animals (Fox, 2002). Rats have 5 rows of whiskers, labeled A–E, which are active tactile detectors. The whiskers are represented in S1 by an isomorphic map of cortical columns, each centered on a cell cluster in layer 4 (L4) called a barrel. L4 excitatory cells in each barrel receive thalamocortical whisker input and make a strong feedforward projection to L2/3 pyramidal cells and inhibitory interneurons in the same column (Feldmeyer et al., 2002; Helmstaedter et al., 2008). Neurons in each column respond most strongly to deflection of the corresponding whisker, resulting in a whisker receptive field map across S1. Plucking or trimming a subset of whiskers in juvenile animals causes whisker map plasticity in which spiking responses to deprived whiskers are rapidly depressed in L2/3 of deprived columns, while responses in L4 remain relatively unaffected (Drew and Feldman, 2009; Feldman and Brecht, 2005; Stern et al., 2001). Such response depression is a common early component of classical Hebbian map plasticity in sensory cortex (Feldman, 2009).

Whisker response depression in L2/3 is mediated by several known changes in excitatory circuits, including long-term depression (LTD) of excitatory L4 synapses onto L2/3 pyramidal cells (Allen et al., 2003; Bender et al., 2006; Shepherd et al., 2003), reduced local recurrent connectivity in L2/3 (Cheetham et al., 2007), and reorganization of L2/3 horizontal projections and projections from L4 interbarrel septa (Broser et al., 2008; Shepherd et al., 2003). However, whether plasticity also occurs within L2/3 inhibitory circuits and how it contributes to the expression of whisker map plasticity remain unknown. We focused on a specific circuit component, feedforward inhibition, because it powerfully sharpens receptive fields, sets response gain and dynamic range, and enforces spike timing precision (Bruno and Simons, 2002; Carvalho and Buonomano, 2009; Gabernet et al., 2005; Miller et al., 2001; Pouille et al., 2009; Pouille and Scanziani, 2001; Swadlow, 2002), suggesting that changes in feedforward inhibition or its balance with excitation may contribute importantly to expression of sensory map plasticity.

We found that the most sensitive L4-L2/3 feedforward inhibition is mediated by L2/3 fast-spiking (FS) interneurons. Whisker deprivation weakened L4 excitatory drive onto L2/3 FS cells, which was partly offset by strengthening of unitary FS to pyramidal cell inhibition. Overall, deprivation strongly reduced net feedforward inhibition. This reduction in feedforward inhibition occurred in parallel with the known reduction in feedforward excitation onto L2/3 pyramidal cells (Allen et al., 2003; Bender et al., 2006; Shepherd et al., 2003) so that the ratio and timing of feedforward excitatory to inhibitory conductance in individual pyramidal cells was maintained. Thus, feedforward inhibition is plastic, and weakening of feedforward inhibition constitutes a compensatory mechanism that can maintain excitatory-inhibitory balance during deprivation-induced Hebbian map plasticity.

RESULTS

We induced whisker map plasticity by plucking the right-side D-row whiskers for 6–12 days, starting at P12, which is a robust early critical period for L2/3 map plasticity (Stern et al., 2001). This deprivation paradigm weakens whisker-evoked spiking responses in L2/3, but not L4, of deprived columns, indicating a locus for plasticity in L4-L2/3 or L2/3 circuits (Drew and Feldman, 2009). To determine whether feedforward inhibition was altered by deprivation, we prepared “across-row” S1 slices in which A–E row whisker columns can be unambiguously identified (Finnerty et al., 1999). We compared synaptic and cellular properties of inhibitory circuits in D whisker columns from deprived animals vs. sham-deprived littermates, except in conductance experiments (see below) where we compared deprived D vs. spared B whisker columns in slices from deprived animals. Spared columns

are appropriate controls because whisker responses and single-cell physiological properties in spared columns are unaffected by D-row deprivation (Allen et al., 2003; Drew and Feldman, 2009).

L4-L2/3 feedforward inhibition is mediated by L2/3 FS interneurons

To measure L4-L2/3 feedforward inhibition, we stimulated L4 extracellularly at low intensity and made whole-cell recordings from co-columnar L2/3 pyramidal cells, with 50 μM D-APV in the bath to reduce polysynaptic excitation. In current clamp, L4 stimulation evoked EPSP-IPSP sequences in L2/3 pyramidal cells (Figure 1B, top). In voltage clamp, L4-evoked inhibitory currents (Cs^+ gluconate internal containing 5 mM BAPTA; 0 mV holding potential) were essentially abolished by 10 μM NBQX, indicating that inhibition was largely polysynaptic (Figure 1B, bottom). We characterized the recruitment of feedforward inhibition by measuring L4-evoked excitation and inhibition in single pyramidal cells at increasing L4 stimulation intensities above excitatory response threshold, defined as the intensity required to evoke an EPSC with no failures (EPSCs measured at −68 mV, IPSCs measured at 0 mV). At each stimulation intensity, mono- and polysynaptic inhibition were separated using NBQX (see Methods). Polysynaptic inhibition was first detectable at 1.2 × excitatory response threshold, and 97 ± 2 % of inhibition was polysynaptic at this intensity (n = 10 cells) (Figure 1C).

To determine whether L4-evoked inhibition was feedforward (as opposed to feedback), we made cell-attached recordings (using K^+ gluconate internal) from L2/3 pyramidal cells and from L2/3 inhibitory interneurons, which provide ~ 80% of inhibitory input onto L2/3 pyramids (Dantzker and Callaway, 2000). We measured spike probability in response to increasing L4 stimulation intensity (measured relative to excitatory response threshold for a co-columnar pyramidal cell), and then broke in to establish whole-cell recording and to classify each cell as a putative pyramidal (PYR) cell, fast-spiking (FS) interneuron or regular spiking non-pyramidal (RSNP) interneuron by electrophysiological criteria (see Suppl. Material and Figure S1). Biocytin reconstruction showed that FS interneurons were primarily basket cells while RSNP cells were bipolar, bitufted and basket cells, and all PYR cells had dense dendritic spines characteristic of excitatory cells (Figure 2A).

We found that L2/3 FS cells were much more likely to spike to low-intensity L4 stimulation than PYR or RSNP cells (Figure 2B). The median stimulation intensity required to reliably evoke ≥ 1 spike was 2.5, 5.0, and 5.5 × excitatory response threshold for FS, RSNP and PYR cell types (Figure 2C) (n = 10, 21 and 22 cells). This is consistent with the strong excitation that L2/3 FS cells receive from L4 excitatory cells (Helmstaedter et al., 2008). Because L2/3 PYR cells did not spike at low stimulation intensity (< 2 × threshold), L4-evoked inhibition at low stimulus intensity must be feedforward rather than feedback inhibition. Additional experiments using 2-photon calcium imaging from large populations of L2/3 pyramidal cells confirmed that L4 stimulation at < 2 × threshold evoked spikes in only 1/110 L2/3 PYR neurons (Elstrott and Feldman, unpublished results). This confirms that low-intensity L4 stimulation selectively evokes feedforward inhibition and excitation onto L2/3 pyramidal cells. Because L4 stimulation primarily activates FS cells among L2/3 interneurons, the most sensitive feedforward inhibition is likely to be mediated by L2/3 FS neurons.

Deprivation depresses L4-evoked excitation onto FS cells

To determine how deprivation affects L4-L2/3 feedforward inhibition, we first assayed L4-evoked excitation onto L2/3 FS cells. L4-evoked EPSPs were recorded in current clamp from L2/3 FS, RSNP and PYR neurons in D columns of D-row deprived rats or whisker-intact, sham-deprived littermates. Focal bicuculline was used to block inhibition and high-

divalent Ringer's (4 mM Ca^{++}, 4 mM Mg^{++}) was used to reduce polysynaptic activity and isolate monosynaptic EPSPs (Allen et al., 2003) (Figure 3A). For each cell, we constructed an input-output curve for EPSP amplitude and initial slope in response to L4 stimulation at 1.0 – 1.8 × excitatory response threshold measured for a co-columnar pyramidal cell. EPSPs were measured at −70 mV in PYR cells, and at −60 mV in FS and RSNP cells (to mimic normal V_{rest}, Figure S1F).

Deprivation substantially reduced input-output curves for L2/3 FS cells (by ~50%) in deprived relative to sham-deprived columns (n = 9 cells each; amplitude: $p < 0.0001$; slope: $p < 0.001$; 2-way ANOVA) (Figure 3B1–2). These changes occurred despite identical stimulation intensity in deprived vs. sham-deprived columns (3.4 ± 0.2 μA and 3.4 ± 0.2 μA at excitatory response threshold, $p = 0.80$, t-test). For PYR cells, deprivation also reduced input-output curves for EPSP amplitude and slope relative to sham-deprived columns (n = 26 and 25 cells each; amplitude: $p < 0.01$; slope: $p < 0.02$) (Figure 3C). This is consistent with known weakening of L4-L2/3 excitatory synapses onto PYR cells (Allen et al., 2003; Bender et al., 2006; Shepherd et al., 2003). For RSNP cells, input-output curves were inconsistently affected, with EPSP amplitude being unchanged in deprived vs. sham-deprived columns (n= 12 and 9 cells), but EPSP slope showing a trend toward decrease (amplitude: $p = 0.54$; slope: $p = 0.05$) (Figure 3D).

Weakening of L4-evoked excitation onto FS cells was confirmed by dual recordings from neighboring PYR and FS cells in the same cortical column (Figure 4A). PYR and FS cells (mean 90 μm, max 170 μm apart) were recorded simultaneously or sequentially, and an input-output curve for EPSPs onto each cell was measured using identical L4 stimulation. In sham-deprived D columns, L4-evoked EPSPs in L2/3 FS cells were reliably larger than EPSPs in co-columnar PYR cells (Figure 4B; shown for 1.4x threshold), as expected for strong, highly sensitive feedforward inhibition (Bruno and Simons, 2002; Helmstaedter et al., 2008; Hull et al., 2009; Swadlow, 2002). However, in deprived D columns, EPSP slope and amplitude were equal or smaller in FS cells compared to co-columnar pyramidal cells (Figure 4B; 1.4x threshold). Across stimulation intensities, FS cells in sham-deprived columns consistently received stronger EPSPs than co-columnar PYR cells, while FS cells in deprived columns received weaker or equal EPSPs than co-columnar PYR cells (Figure 4C) (n = 9 each; amplitude, $p < 0.001$, 2-way ANOVA, slope, $p < 0.0001$).

These findings demonstrate that deprivation weakens L4 excitation onto L2/3 FS cells even more substantially than the previously known weakening of L4 excitation onto L2/3 PYR cells (Allen et al., 2003; Bender et al., 2006; Shepherd et al., 2003). This suggests that deprivation reduces the recruitment of L2/3 feedforward inhibition onto L2/3 pyramidal cells.

Deprivation does not change the intrinsic excitability of FS cells

To test whether deprivation altered FS excitability, we first measured passive membrane properties and intrinsic spiking of L2/3 FS cells in D columns of deprived rats and sham-deprived littermates. In whole-cell recordings, resting membrane potential (V_m), input resistance (R_{in}), membrane time constant (τ), and spike threshold were identical in deprived vs. sham-deprived columns, as was spiking rate in response to 500-ms somatic current injection (n = 21 sham, 20 deprived) (Figure 5A,B).

To assess synaptically driven excitability, we measured the magnitude of L4 excitatory synaptic input required to drive spikes in L2/3 FS cells. Recording in cell-attached mode (K^+ gluconate internal, 50 μM APV in bath), we first determined the L4 stimulation intensity required to elicit 50% (range: 40–60%) spiking probability (Figure 5C). Then, we broke in and measured in voltage clamp the L4-evoked excitatory conductance at this stimulation

intensity, termed threshold G_e (see Methods). Threshold G_e represents the magnitude of excitation required to elicit 50% spike probability. Deprivation did not alter integrated threshold G_e (calculated from response onset to each cell's mean spike latency) or peak, indicating that the amount of excitatory drive necessary to elicit a spike from V_{rest} was unaltered (n = 8 sham, 6 deprived) (Figure 5D and Figure S2). Together, these results indicate that FS cell intrinsic excitability is essentially unaltered after deprivation. However, deprivation did increase onset latency of threshold G_e (sham-deprived, 3.3 ± 0.3 ms, deprived, 4.4 ± 0.2 ms, $p < 0.05$) with a corresponding increase in evoked spike latency (7.8 ± 0.5 ms vs. 11.1 ± 1.4 ms, $p < 0.05$) (Figure S2).

Potentiation of FS cell unitary amplitude by deprivation

In L4 of visual cortex, sensory deprivation has been reported to enhance inhibition by potentiation of inhibitory FS→PYR synapses (Maffei et al., 2006). To test whether L2/3 FS→PYR synapses are also altered by whisker deprivation, we measured connectivity rate and synapse properties for unitary inhibitory connections from L2/3 FS cells to PYR cells (L2/3 FS→PYR synapses) in D columns from deprived and sham-deprived rats (Figure 6A). Cells were patched with a low chloride internal (E_{Cl} = −88 mV) to increase the size of hyperpolarizing unitary IPSPs (uIPSPs) (Figure 6B). FS spikes were elicited by current injection, and connected FS→PYR pairs were identified by a statistically significant uIPSP amplitude compared to a pre-spike baseline period (20–40 sweeps, post PYR cell V_m = −50 mV, paired sign rank test, $p < 0.05$).

The L2/3 FS→PYR connection rate was greater in deprived columns (22/28 pairs connected, 78.6% connection rate [95% confidence interval 61–93%] vs. sham-deprived columns (21/45 pairs connected, 46.7% [31–60%]; $p < 0.01$, ranksum test). Intersoma distance was identical for these connected pairs (deprived, 54 ± 5 μm, sham-deprived, 51 ± 5 μm). FS→PYR uIPSP amplitude for connected pairs was also greater in deprived (−1.59 ± 0.23 mV, n = 21 pairs, measured at V_m = −50 mV) than in sham-deprived columns (−0.69 ± 0.12 mV, n = 20, $p < 0.01$, t-test; one pair in each condition excluded because of low R_{in}). uIPSP slope was similarly increased (deprived: −0.27 ± 0.05 mV/ms, sham-deprived: −0.12 ± 0.02 mV/ms, $p < 0.01$) (Figure 6B–D). This increase in uIPSP synapse strength and connection rate was associated with a decrease in failure rate (deprived, 16.3 % [8–30%], sham-deprived, 36.8 [22–52%], $p < 0.04$, ranksum test) and coefficient of variation (deprived, 0.27 [0.22–0.37], sham-deprived, 0.40 [0.30–0.69], $p < 0.05$, ranksum test). Deprivation did not alter short-term plasticity during trains of 5 presynaptic spikes (50 ms isi) or uIPSP kinetics (Figure 6E–F). Together, these results suggest that deprivation strengthens uIPSPs by increasing the number of synapses or release sites.

Deprivation reduces L4-evoked feedforward inhibition onto L2/3 pyramidal cells

If deprivation weakens L4 excitation onto L2/3 FS neurons, but increases FS→PYR unitary synapse strength, what is the overall net effect of deprivation on feedforward inhibition? To address this, we measured net L4-evoked feedforward inhibition and excitation onto single L2/3 pyramidal cells in voltage clamp (Cs^+ gluconate internal with 5 mM BAPTA, 50 μM APV in bath to reduce polysynaptic excitation). L4 stimulation intensity was standardized at 1.2 times excitatory response threshold, in order to study the initial recruitment of feedforward inhibition (Figure 1C). We measured currents at multiple holding potentials and calculated L4-evoked excitatory and inhibitory conductance (G_e and G_i) using standard estimation techniques (Wehr and Zador, 2003). Most cells showed a small, rapid G_e waveform simultaneous with, or followed by, a larger G_i waveform (Figures 7A–B).

Calibration experiments showed that conductance estimation was reasonably accurate for L4-evoked input to L2/3 PYR cells, which occurs at proximal synapses (FS-mediated

inhibition at the soma, excitation on proximal basal dendrites an average of 62 μm from the soma (Lubke et al., 2003)). L4-evoked synaptic currents showed a linear I–V relationship at holding potentials ≤ 0 mV (Figure S3A and S3B) even without QX-314 to block sodium channels (Figure S3C). This suggests adequate voltage clamp. We tested the accuracy of conductance estimation using a multicompartment NEURON model of a passive L2/3 PYR cell (Traub et al., 2003) with resting conductance, membrane capacitance and R_{series} calibrated to match L2/3 PYR cells in our slice experiments (P18-24, 23°C, APV to block NMDA receptors) (Figure S4). Inhibitory and excitatory synaptic conductances were placed at the soma and 62 μm along a basal dendrite (5:1 amplitude ratio, with inhibition at a 2 ms delay). We simulated somatic voltage clamp measurements at different holding potentials, and estimated G_e and G_i using the conductance estimation method. For realistic size conductances (1 nS G_e and 5 nS G_i), the method recovered 47% and 71% of peak G_e and G_i, respectively, and 87% and 97% of integrated G_e and G_i. Accuracy dropped modestly with synapse distance from soma (Figure S4B). Thus, despite space clamp and voltage escape errors for large pyramidal cells (Poleg-Polsky and Diamond, 2011; Williams and Mitchell, 2008), voltage clamp-based conductance estimation is reasonable for proximal excitatory and inhibitory inputs onto moderate-sized L2/3 pyramidal cells under *in vitro* conditions, particularly for integrated conductance.

We compared G_i and G_e between deprived D columns and spared B columns in slices from whisker-deprived rats, using L4 stimulation at 1.2 x threshold (Figure 7C–F). Results showed that peak G_i and integrated G_i (first 20 ms) were reduced substantially in deprived columns relative to spared columns (peak: 2.56 ± 0.47 nS vs. 5.98 ± 1.56 nS, n = 37 each, $p < 0.05$; integrated: 33.27 ± 6.0 nS × ms vs. 77.04 ± 19.4 nS × ms, $p < 0.05$, unpaired t-test). Thus, deprivation reduces overall feedforward inhibition onto pyramidal cells. Peak G_e was also lower in deprived columns (deprived: 0.99 ± 0.11 nS, n = 37 cells; spared: 1.51 ± 0.23 nS, n = 37 cells; $p < 0.05$), and integrated G_e showed similar but non-significant weakening (deprived: 7.32 ± 0.9 nS × ms; spared: 9.67 ± 1.3 nS × ms; p = 0.13). EPSC paired pulse ratio was also increased (deprived: 1.29 ± 0.07; spared: 1.09 ± 0.06; $p < 0.05$, 40 ms interval, measured at $E_{Cl} = -68$ mV). These findings are consistent with the known presynaptic weakening of L4 excitatory synapses onto L2/3 pyramidal cells (Allen et al., 2003; Bender et al., 2006). These changes in G_i and G_e were not due to differences in L4 stimulation intensity in deprived vs. spared columns (7.2 ± 0.8 μA and 8.1 ± 0.9 μA excitatory response threshold, p = 0.47) and are unlikely to reflect differential space clamp errors because passive and active electrical properties are unaltered by deprivation (Allen et al., 2003). Peak G_e and G_i were identical between spared columns in deprived rats and control D columns in whisker-intact rats (peak G_e: 1.31 ± 0.15 nS; peak G_i: 5.53 ± 1.67 nS; n = 15), confirming that spared columns are unaffected by this deprivation protocol (Allen et al., 2003; Drew and Feldman, 2009). Thus, deprivation reduced L4-evoked feedforward inhibition and feedforward excitation onto L2/3 pyramidal cells.

Deprivation weakens feedforward inhibition and excitation in parallel

The ratio of excitation to inhibition onto single neurons critically shapes input-output gain, dynamic range, receptive field sharpness, and spiking probability (Carvalho and Buonomano, 2009; Miller et al., 2001; Pouille et al., 2009; Pouille and Scanziani, 2001). We quantified the relative magnitude of G_e vs. G_i in single cells as $G_e / (G_e + G_i)$, termed G_e fraction. G_e fraction was broadly distributed (Figure 8A), reflecting only a weak correlation between G_e and G_i in individual cells ($r^2 = 0.438$ for 37 spared and 37 deprived cells, but $r^2 = 0.059$ [p = 0.04] if 2 cells with largest G_e and G_i are excluded). Deprivation reduced mean G_e without altering the distribution, mean, or median G_e fraction (Figure 8B–C). This was true whether G_e fraction was calculated either from peak G_e and G_i (deprived: 0.45 ± 0.05, spared: 0.43 ± 0.05, mean ± SEM, p = 0.78) or from integrated G_e and G_i (deprived: 0.37 ±

0.05, spared: 0.35 ± 0.05, p = 0.76). Thus, whisker deprivation drives a strong, coordinated decrease of excitation and inhibition onto L2/3 pyramidal cells, in which the relative magnitude of excitation vs. inhibition remains constant across the L2/3 neuron population.

Deprivation delays synaptic responses but preserves excitatory-inhibitory timing

To test whether deprivation altered the relative timing of excitation and inhibition, which provides a critical temporal filter for postsynaptic integration and spiking (Gabernet et al., 2005; Pouille and Scanziani, 2001; Wilent and Contreras, 2005), we measured latencies to onset, 50% peak conductance, and peak conductance for L4-evoked G_e and G_i in each neuron. Deprivation delayed G_e and G_i onset by 0.73 and 1.1 ms, respectively, and delayed G_e and G_i peaks by 1.1 and 1.5 ms (Figure 8D; Table S1). Within single cells, deprivation did not significantly affect the relative latency from G_e onset to G_i onset (p = 0.10). The temporal evolution of G_e fractional conductance was also unchanged by deprivation (Figure 8E). Thus, deprivation delayed both excitation and inhibition to L2/3 pyramids, but generally preserved the relative timing of these signals. The overall delay in synaptic input may explain the increased spike latency in L2/3 neurons after D-row deprivation *in vivo* (Drew and Feldman, 2009). The delay in L4-evoked inhibition may be attributable to delayed spiking in L2/3 FS cells (Figure S2C and S2D).

Functional effect of parallel inhibitory and excitatory weakening

Reduction of excitation is expected to decrease L4-evoked synaptic potentials in L2/3 pyramids while reduction of inhibition may increase them. To test the overall functional effect of co-reduction of G_e and G_i on L4-evoked synaptic depolarization in L2/3 pyramids, we used a single-compartment parallel conductance model (Wehr and Zador, 2003) to predict the net PSP produced by the G_e and G_i waveforms measured in each pyramidal cell (Figures 7-8). The model calculates the PSP produced by G_e and G_i waveforms at a specific baseline V_m, given excitatory and inhibitory reversal potentials (E_e = 0 mV, E_i = -68 mV) and standardized input resistance (214 MΩ) and membrane capacitance (0.19 nF). Running the model for all cells predicted a broad distribution of peak PSP depolarization above baseline (ΔV_m) reflecting the cell-to-cell heterogeneity in measured G_e and G_i waveforms. However, the largest ΔV_m values were reduced in deprived columns relative to spared columns (Figure S5). Thus, this simple model indicates that the measured co-reduction in inhibition and excitation will lead to a net reduction in maximal feedforward activation of L2/3 pyramids.

DISCUSSION

Down-regulation of neural responses to deprived sensory inputs is a major component of map plasticity in juvenile animals (Feldman and Brecht, 2005), but how plasticity of inhibitory circuits contributes to this phenomenon remains incompletely understood. We assayed plasticity of feedforward inhibitory circuits and excitatory-inhibitory balance in L2/3 of S1, which is the major site of deprivation-induced plasticity in post-neonatal animals (Fox, 2002). Prior studies focused almost exclusively on excitatory circuit mechanisms for L2/3 plasticity, which include weakening of L4 feedforward excitation and reduced recurrent excitation onto L2/3 pyramidal cells (Allen et al., 2003; Bender et al., 2006; Cheetham et al., 2007; Shepherd et al., 2003). In V1, monocular lid suture alters sensory response properties of L2/3 inhibitory neurons, suggesting that plasticity in L2/3 also involves changes in inhibition (Gandhi et al., 2008; Kameyama et al., 2010; Yazaki-Sugiyama et al., 2009), but the synaptic changes in L2/3 inhibitory circuits that mediate this effect have not yet been identified (Maffei and Turrigiano, 2008).

Feedforward inhibition is a major circuit motif in cerebral cortex that powerfully regulates sensory responsiveness in S1 (Gabernet et al., 2005; Miller et al., 2001; Wilent and Contreras, 2005), including sharpening receptive fields (Bruno and Simons, 2002; Foeller et al., 2005), improving spike timing precision necessary for coding natural whisker inputs (Gabernet et al., 2005; Jadhav et al., 2009), setting input-output gain and dynamic range (Carvalho and Buonomano, 2009; Pouille et al., 2009). Experience-dependent regulation of inhibition could help optimize these aspects of sensory coding during L2/3 circuit development. We found that low-threshold L4-L2/3 feedforward inhibition is mediated by L2/3 FS interneurons, similar to L4 of S1 and hippocampus. In these structures, FS neurons mediate sensitive and powerful feedforward inhibition due to intense excitation from feedforward inputs, a high connection rate, and strong perisomatic synapses onto target pyramidal cells (Cruikshank et al., 2007; Gabernet et al., 2005; Hull et al., 2009). These same properties are true of FS cells in L2/3 of S1 (Figures 4, 6) (Galarreta et al., 2008; Helmstaedter et al., 2008; Kapfer et al., 2007), and FS cells are preferentially recruited to spike by low-intensity L4 activation (Figure 2). FS cells are also excited by L2/3 pyramidal cells, indicating that they also contribute to feedback inhibition, which was not studied here (Galarreta et al., 2008; Reyes et al., 1998).

Deprivation weakens feedforward inhibition by FS circuits

The deprivation protocol used here, 6–12 days of D-row whisker deprivation, drives robust Hebbian weakening of deprived whisker responses in L2/3 *in vivo* (Drew and Feldman, 2009). We found that whisker deprivation caused a substantial reduction in L4-evoked excitation onto L2/3 FS cells in deprived cortical columns, which was partially offset by an increase in unitary IPSPs from L2/3 FS cells to pyramidal cells. Deprivation did not alter FS intrinsic excitability, unlike in L4 of S1 (Sun, 2009). The net effect of these cellular changes was an overall reduction in L4-evoked feedforward inhibitory conductance in L2/3 pyramidal cells compared to spared columns (Figure 7). Thus, Hebbian weakening of deprived whisker responses in L2/3 of S1 involves weakening of FS-mediated feedforward inhibition. This is unlike in L4 of V1, where visual deprivation during the critical period also potentiates unitary FS→principal cell inhibitory synapses, which is proposed to suppress responses to the deprived eye (Maffei et al., 2006). In S1, deprivation during the critical period potentiates FS→PYR uIPSPs, but a more substantial reduction in L4 drive onto FS cells results in a significant net decrease in feedforward inhibition.

The cellular mechanisms for these changes are not known but could include impaired development, removal, or long-term depression (LTD) of excitatory synapses on FS cells (Kullmann and Lamsa, 2007; Lu et al., 2007), and synaptogenesis or inhibitory LTP (Holmgren and Zilberter, 2001; Knott et al., 2002; Maffei et al., 2006; Marik et al., 2010) of GABAergic FS output synapses. These findings add to increasing evidence that FS cells are a site of robust experience-dependent development and plasticity *in vivo* (Chittajallu and Isaac, 2011; Gandhi et al., 2008; Jiao et al., 2006; Maffei et al., 2006; Maffei et al., 2004; Yazaki-Sugiyama et al., 2009).

Balanced weakening of inhibition and excitation

Prior work showed that D-row deprivation reduces feedforward and recurrent excitation into L2/3 of deprived columns (Allen et al., 2003; Bender et al., 2006; Cheetham et al., 2007; Shepherd et al., 2003), but whether plasticity was coordinated between excitatory and inhibitory circuits was unknown. Because sensory responses in cortical neurons depend strongly on the balance and timing of convergent excitation and inhibition (Pouille et al., 2009; Wehr and Zador, 2003; Wilent and Contreras, 2005), we simultaneously measured L4-evoked feedforward inhibition and excitation onto single L2/3 pyramidal cells, and found that 6–12 days of D-row deprivation caused a co-reduction in excitation and inhibition

in which the ratio of excitation to inhibition in single cells was preserved, on average, in the population, relative to spared columns (Figure 8). Deprivation delayed both excitation and inhibition by ~ 1 ms, but did not alter their relative timing. Thus, Hebbian weakening of deprived inputs in S1 is associated with a coordinated decrease and delay in feedforward excitation and inhibition.

Most neurons in L2/3 of S1 respond to whisker deflection with subthreshold depolarization, reflecting sparse spike coding in this region (Crochet et al., 2011). To understand how co-reduction of excitation and inhibition affects L4-evoked subthreshold responses, we used a single-compartment parallel conductance model (Wehr and Zador, 2003) to predict the PSP produced by the measured L4-evoked G_e and G_i waveforms measured in each pyramidal cell. This model showed that the measured co-reduction in feedforward excitation and inhibition will produce a net decrease in L4-evoked PSP amplitude (Figure S5). Thus, this effect is appropriate to explain the Hebbian weakening of L2/3 responses to deprived whiskers. Additional factors mediating reduced L2/3 spiking probability *in vivo* may include nonlinear amplification of PSP weakening by the spike threshold (Foeller et al., 2005; Priebe and Ferster, 2008), reduced L2/3 recurrent excitation (Cheetham et al., 2007), or potential changes in feedback inhibition. While the reduction in feedforward excitation is predicted to decrease PSP amplitude, the reduction in feedforward inhibition is expected to increase PSP amplitude, and therefore represents a partial, covert compensatory mechanism. This compensation is termed ‘covert’ because it does not result in increased whisker-evoked or spontaneous spikes *in vivo* (Drew and Feldman, 2009).

How coordinated weakening of inhibition and excitation is achieved is an important topic for future work. A simple passive process in which L4 neurons reduce synaptic strength equally onto FS and PYR target neurons is not supported by our data, because L4→FS excitation must weaken disproportionately to offset the strengthening of FS→PYR uIPSPs by deprivation (Fig. 4B, Fig. 6). Instead, we propose that an active process exists to establish and maintain an appropriate average balance and timing between excitation and inhibition in L2/3 PYR cells. A similar active process may occur in L4 of S1, where feedforward excitatory synapses onto both pyramidal and FS cells are also co-regulated by sensory experience during development (Chittajallu and Isaac, 2011). The mechanisms for active balancing are unclear, and could involve activity-dependent regulation of excitatory synapse development onto FS cells (e.g., by Narp Chang et al., 2010) or of inhibitory synapse development onto PYR cells (e.g. by Npas-4 or BDNF Hong et al., 2008; Jiao et al., 2011; Lin et al., 2008), or associative plasticity at input or output synapses of FS cells (Lu et al., 2007; Maffei et al., 2004).

Potential roles for reduced inhibition during whisker map plasticity

Reduced feedforward inhibition could perform multiple roles in Hebbian map plasticity. First, it may act as a compensatory mechanism to increase cortical responsiveness in response to decreased sensory drive. Consistent with this view, most previous examples of sensory-driven plasticity of S1 inhibitory circuits are compensatory in sign (Feldman, 2009). This includes in L4, where whisker deprivation reduces IPSC amplitude (Jiao et al., 2006), FS excitability (Sun, 2009), inhibitory synapse density (Micheva and Beaulieu, 1995) and GABA-A receptor expression (Fuchs and Salazar, 1998), whereas whisker stimulation drives inhibitory synaptogenesis and increased inhibitory marker expression (Jasinska et al., 2010; Knott et al., 2002). Compensation by altered inhibition is distinct from homeostatic synaptic scaling of excitation or regulation of intrinsic excitability in PYR cells, which have only been observed *in vivo* during distinct homeostatic phases of plasticity, not during classical Hebbian plasticity (Maffei et al., 2010; Turrigiano and Nelson, 2000). Reduced inhibition could therefore fulfill theoretical predictions for compensatory or homeostatic

plasticity that coexists with Hebbian plasticity to stabilize cortical function during map plasticity (Mrsic-Flogel et al., 2007; Turrigiano and Nelson, 2004).

A second potential role for reduced inhibition may be as a permissive gate to enable subsequent components of map plasticity, including use-dependent increase of spared whisker responses or recovery of responses to regrown whiskers. For example, reduced inhibition promotes LTP (Wigstrom and Gustafsson, 1986), which may promote later potentiation of spared whisker responses. Deprivation-induced changes in inhibition have been similarly proposed to enable later components of plasticity in V1 (Gandhi et al., 2008; Yazaki-Sugiyama et al., 2009).

Perhaps most importantly, the reduction in feedforward inhibition may serve to ensure that excitation and inhibition remain balanced during whisker map plasticity. From a sensory processing point of view, this would be highly advantageous, since the ratio and timing of excitation to inhibition onto single neurons are critical for sensory information processing including setting receptive field sharpness, input-output gain, dynamic range and spike timing precision (Carvalho and Buonomano, 2009; Gabernet et al., 2005; Miller et al., 2001; Pouille et al., 2009; Pouille and Scanziani, 2001). Maintenance of excitation-inhibition balance may therefore function to maintain normal sensory processing during map plasticity. This may be particularly important in S1, where processing must be maintained as whiskers are shed and regrow throughout life. Preservation of excitation-inhibition balance also appears important in auditory cortex, where excitation and inhibition are transiently unbalanced and then rebalanced onto single neurons during development and some forms of plasticity (Dorrn et al., 2010; Froemke et al., 2007). However, it may be less relevant in visual cortex, where excitation-inhibition balance is not maintained during visual deprivation (Maffei et al., 2004; 2006; 2008).

Summary

The loss of responses to deprived whiskers is accompanied by a parallel decrease in feedforward inhibition and excitation onto L2/3 pyramids. The covert reduction of feedforward inhibition is a previously unknown component of Hebbian map plasticity in S1, and we propose that it may act to compensate for reduced sensory drive, to maintain excitation-inhibition balance necessary for basic feedforward sensory computation, and to enable later stages of excitatory plasticity including restoring function after whisker regrowth. The maintenance of excitation-inhibition balance after deprivation suggests that mechanisms exist to preserve this balance, which is a critical feature of normal cortical function and whose dysregulation may contribute to epilepsy, autism, and other disorders (Rubenstein and Merzenich, 2003).

METHODS

Experiments used Long-Evans rats. Procedures were approved by UCSD and UC Berkeley Institutional Animal Care and Use Committees and are in accordance with NIH guidelines.

Whisker deprivation

Starting at postnatal day (P) 12, D-row whiskers D1–D6 and γ were plucked from the right side of the face under transient isoflurane anesthesia (3.5% in 3L/min O_2). Plucking continued every other day until recording. Sham-plucked rats were anesthetized but not plucked.

Slice Preparation

P18-24 rats were anesthetized with isoflurane, the brain was quickly removed, and slices were cut on a vibratome (Leica VT1000S). Slices were prepared in either chilled normal Ringer's solution (mM: 119 NaCl, 26.2 $NaHCO_3$, 11 D-(+)-glucose, 1.3 $MgSO_4$, 2.5 KCl, 1 NaH_2PO_4, 2.5 $CaCl_2$, bubbled with 95% O_2/5% CO_2, pH 7.30, 310 mOsm), low-sodium, low-calcium, HEPES-buffered cutting solution (mM: 250 Sucrose, 15 HEPES, 11 D-(+)-glucose, 4 $MgSO_4$, 2.5 KCl, 1 NaH_2PO_4, 0.1 $CaCl_2$), or low-sodium, low-calcium, bicarbonate buffered cutting solution (mM: 85 NaCl, 75 Sucrose, 25 D-(+)-glucose, 4 $MgSO_4$, 2.5 KCl, 1.25 $Na_2HPO_4{*}H_2O$, 0.5 ascorbic acid, 25 $NaHCO_3$, 0.5 $CaCl_2$). Cortical slices (400 μm thickness) were cut from the left hemisphere in the "across-row plane", oriented 50° towards coronal from the midsaggital plane. These slices contain one barrel column from each whisker row (A–E) (Allen et al., 2003; Finnerty et al., 1999). Slices were transferred to normal Ringer's solution and incubated for 30 min at 30° C and 1–6 hr at room temperature before recording. Barrels were visualized by transillumination.

Electrophysiology

Recordings were made at room temperature (22–24°C) with 3–6 MΩ pipettes using Multiclamp 700A, 700B, or Axopatch 200B amplifiers (Molecular Devices, Sunnyvale CA). A bipolar stimulating electrode (FHC, Bowdoin ME) was placed in the center of a L4 barrel. L2/3 neurons in the same radial column were selected for recording.

Current clamp recordings were made using K gluconate internal (mM: 116 K gluconate, 20 HEPES, 6 KCl, 2 NaCl, 0.5 EGTA, 4 MgATP, 0.3 NaGTP, 5 Na_2phosphocreatine, pH 7.2, 295 mOsm). In a subset of cells, biocytin (0.26 %) replaced phosphocreatine to allow morphological reconstruction. Input resistance (R_{input}) was measured with a 120-ms hyperpolarizing current injection in each sweep. Series resistance (R_{series}) was compensated by bridge balance. Cells were excluded if initial R_{series} was > 20 MΩ or if R_{input} or R_{series} changed by > 30% during recording. Sweeps were collected at 10 s intervals.

Voltage clamp recordings were made using Cs gluconate internal (mM: 108 D-gluconic acid, 108 CsOH, 20 HEPES, 5 tetraethylammonium-Cl, 2.8 NaCl, 0.4 EGTA, 4 MgATP, 0.3 NaGTP, 5 BAPTA, pH 7.2, 295 mOsm). R_{input} and R_{series} were monitored in each sweep in response to a 5-mV test pulse. R_{series} was not compensated. Pyramidal cells were excluded if V_m at break-in was > -68 mV, R_{series} > 25 MΩ or R_{input} < 100 MΩ. V_m values for voltage clamp recordings were corrected for the measured liquid junction potential (10–12 mV), while those for current clamp recordings were not. Data acquisition and analysis used custom software in IGOR Pro (Wavemetrics, Portland, OR).

For L4 stimulation, excitatory response threshold was defined as the L4 stimulation intensity that elicited EPSCs with no failures at E_{Cl} (−68 mV). To separate monosynaptic from polysynaptic inhibition (Figure 1), we first recorded the total L4-evoked IPSC (Cs internal with 5 mM BAPTA, V_{hold} = 0 mV, 50 μM APV in the bath), applied 10 μM NBQX to record the monosynaptic IPSC, and then calculated the polsynaptic IPSC by subtraction.

For cell-attached recording of synaptically evoked spikes, neurons were patched in voltage-clamp mode with K^+ internal solution. To avoid biasing the cell's V_m (and therefore its excitability), holding potential (V_{hold}) was adjusted so that $I_{hold} \approx 0$ pA. Capacitative action currents were recorded in the intact patch. After cell-attached recording, we broke in and measured spiking patterns in current clamp mode to classify the cell physiologically as FS or RSNP.

Synaptic conductance measurement

To measure L4-evoked synaptic conductances, recordings were made in voltage clamp using normal Ringer's with 50 μM APV (Tocris), and Cs gluconate internal with 5 mM BAPTA (Sigma-Aldrich). Mean R_{series} and R_{input} were 10.8 ± 0.4 MΩ and 401 ± 24 MΩ. As before, excitatory response threshold was the stimulus intensity necessary to evoke a discernible EPSC in a L2/3 pyramidal cell without failures. An average L4-evoked PSC (6–10 repetitions, 10 s interval) was measured at 1.2 times excitatory response threshold at −90, −68, −40 and 0 mV holding potentials.

L4-evoked excitatory and inhibitory synaptic conductance was calculated using published methods (Wehr and Zador, 2003). First, total synaptic conductance (G_{syn}) and the synaptic reversal potential (E_{rev}) were calculated at each time point, by linear fit to the equation:

$$I_{syn}(t)=G_{syn}(t) * (V_{hold} - E_{rev}(t))$$

G_i and G_e were then calculated based on the measured reversal potentials for excitation (E_e = 0 mV) and inhibition (E_i = −68 mV):

$$G_i(t)=G_{syn}(t) * (E_e - E_{rev}(t))/(E_e - E_i)$$
$$G_e(t)=G_{syn}(t) - G_i(t)$$

E_e and E_i were directly measured in separate voltage clamp experiments from pharmacologically isolated EPSCs (in 50 μM D-APV and 100 μM picrotoxin) and IPSCs (in 50 μM D-APV and 10 μM DNQX). This calculation assumes an isopotential neuron.

Peak conductance was averaged in a 2 ms window. Latency was calculated relative to L4 stimulus onset, unless otherwise stated.

For experiments measuring threshold G_e required to evoke 50% spike probability in FS cells (Figure 5), L4-evoked EPSCs were recorded near the reversal potential for inhibition. G_e was calculated at this single holding potential, based on the driving force for excitation: $G_e = I / (V_{hold} - E_e)$.

Intrinsic excitability

Immediately after break-in, V_{rest} was measured, and R_{input} and membrane time constant were measured from the V_m response to a 500 ms negative current injection. The current-firing rate relationship was measured by injecting 500-ms depolarizing current in steps from rheobase (minimum current to elicit at least one spike) to rheobase + 200 pA, in steps of 20 pA. Spike threshold was determined at rheobase + 40 pA injected current as the prespike V_m at which dV/dt > 10 mV/ms.

Interneuron and pyramidal cell classification

L2/3 pyramidal cells were identified by soma shape under DIC optics. All suspected pyramidal cells showed regular spiking patterns in current clamp, and had dendritic spines in recovered biocytin fills (12/12 neurons). Cells with non-pyramidal somata were classified as RSNP or FS interneurons based on spike frequency adaptation in response to 500-ms current injection (Figure S1). Average spike frequency adaptation (α_{avg}) was defined as the last interspike interval divided by the first interspike interval, averaged over all spike trains in response to current injections from rheobase to rheobase + 200 pA. FS interneurons were defined as cells with $\alpha_{avg} < 1.5$, and RSNP cells as having $\alpha_{avg} > 1.5$. All pyramidal cells

had $\alpha_{avg} \gg 1.5$. Of 16 FS cells that were recovered in biocytin reconstructions with sufficient axonal staining for morphological classification, 11 were small or nest basket cells and 5 were large basket cells. Of 8 RSNP cells recovered in biocytin reconstructions, 2 were small basket cells, 4 were bipolar or bitufted cells, 1 was a large basket cell, and 1 was a neurogliaform cell, reflecting the heterogeneity of our electrophysiological classification of RSNP cells.

Histological reconstruction

In a subset of cells, biocytin immunostaining was performed as published previously (Bender et al., 2003). Neurons were reconstructed using brightfield imaging on an Axioskop 2 plus microscope (Carl Zeiss, Thornwood NY) and Neurolucida software (Microbrightfield, Williston VT).

FS-PYR cell pairs

Connectivity was tested between FS and PYR cells with intersoma distance < 150 μm. FS and PYR cells were recorded with modified K gluconate internal (2 mM KCl, 120 mM K gluconate) with $E_{Cl} = -88$ mV. PYR V_m was maintained at −50 mV using the “slow” current clamp function of the Multiclamp 700B (at the 5 second setting). In each sweep (10 sec isi), an FS spike was elicited by a 3-ms current pulse (0.5–1 nA). Existence of a connection was evaluated from 20–40 sweeps. uIPSP amplitude (defined as average amplitude in a 10 ms window at IPSP peak), initial slope (first 4 ms), failure rate and coefficient of variation were measured from 30–40 sweeps. Failures were defined as responses with amplitude < 2 standard deviations above the average baseline noise. Coefficient of variation was calculated from adjusted variance (uIPSP amplitude variance – noise variance measured in a prestimulus window).

Statistics

Reported values are mean ± SEM unless otherwise noted. 95% confidence intervals were generated by resampling the original distributions and applying the bias-corrected percentile method (Efron and Tibshirani, 1991).

Supplementary Material

Refer to Web version on PubMed Central for supplementary material.

Acknowledgments

We thank Massimo Scanziani for experiment suggestions, Chloe Thomas and Luke Bogart for histology assistance, and Kevin Bender for pyramidal cell reconstruction. Supported by NIH 2R01 NS046652 and 1R01 NS073912, and the Mary Elizabeth Rennie Endowment for Epilepsy at UC Berkeley.

References

Allen CB, Celikel T, Feldman DE. Long-term depression induced by sensory deprivation during cortical map plasticity in vivo. Nat Neurosci. 2003; 6:291–299. [PubMed: 12577061]

Bender KJ, Allen CB, Bender VA, Feldman DE. Synaptic basis for whisker deprivation-induced synaptic depression in rat somatosensory cortex. J Neurosci. 2006; 26:4155–4165. [PubMed: 16624936]

Bender KJ, Rangel J, Feldman DE. Development of columnar topography in the excitatory layer 4 to layer 2/3 projection in rat barrel cortex. J Neurosci. 2003; 23:8759–8770. [PubMed: 14507976]

Broser P, Grinevich V, Osten P, Sakmann B, Wallace DJ. Critical period plasticity of axonal arbors of layer 2/3 pyramidal neurons in rat somatosensory cortex: layer-specific reduction of projections into deprived cortical columns. Cereb Cortex. 2008; 18:1588–1603. [PubMed: 17998276]

Bruno RM, Simons DJ. Feedforward mechanisms of excitatory and inhibitory cortical receptive fields. J Neurosci. 2002; 22:10966–10975. [PubMed: 12486192]

Carvalho TP, Buonomano DV. Differential effects of excitatory and inhibitory plasticity on synaptically driven neuronal input-output functions. Neuron. 2009; 61:774–785. [PubMed: 19285473]

Chang MC, Park JM, Pelkey KA, Grabenstatter HL, Xu D, Linden DJ, Sutula TP, McBain CJ, Worley PF. Narp regulates homeostatic scaling of excitatory synapses on parvalbumin-expressing interneurons. Nat Neurosci. 2010; 13:1090–1097. [PubMed: 20729843]

Cheetham CE, Hammond MS, Edwards CE, Finnerty GT. Sensory experience alters cortical connectivity and synaptic function site specifically. J Neurosci. 2007; 27:3456–3465. [PubMed: 17392462]

Chittajallu R, Isaac JT. Emergence of cortical inhibition by coordinated sensory-driven plasticity at distinct synaptic loci. Nat Neurosci. 2011; 13:1240–1248. [PubMed: 20871602]

Crochet S, Poulet JF, Kremer Y, Petersen CC. Synaptic mechanisms underlying sparse coding of active touch. Neuron. 2011; 69:1160–1175. [PubMed: 21435560]

Cruikshank SJ, Lewis TJ, Connors BW. Synaptic basis for intense thalamocortical activation of feedforward inhibitory cells in neocortex. Nat Neurosci. 2007; 10:462–468. [PubMed: 17334362]

Dantzker JL, Callaway EM. Laminar sources of synaptic input to cortical inhibitory interneurons and pyramidal neurons. Nat Neurosci. 2000; 3:701–707. [PubMed: 10862703]

Dorrn AL, Yuan K, Barker AJ, Schreiner CE, Froemke RC. Developmental sensory experience balances cortical excitation and inhibition. Nature. 2010; 465:932–936. [PubMed: 20559387]

Drew PJ, Feldman DE. Intrinsic signal imaging of deprivation-induced contraction of whisker representations in rat somatosensory cortex. Cereb Cortex. 2009; 19:331–348. [PubMed: 18515797]

Efron B, Tibshirani R. Statistical data analysis in the computer age. Science. 1991; 253:390–395. [PubMed: 17746394]

Feldman DE. Synaptic mechanisms for plasticity in neocortex. Annu Rev Neurosci. 2009; 32:33–55. [PubMed: 19400721]

Feldman DE, Brecht M. Map plasticity in somatosensory cortex. Science. 2005; 310:810–815. [PubMed: 16272113]

Feldmeyer D, Lubke J, Silver RA, Sakmann B. Synaptic connections between layer 4 spiny neurone-layer 2/3 pyramidal cell pairs in juvenile rat barrel cortex: physiology and anatomy of interlaminar signalling within a cortical column. J Physiol. 2002; 538:803–822. [PubMed: 11826166]

Finnerty GT, Roberts LS, Connors BW. Sensory experience modifies the short-term dynamics of neocortical synapses. Nature. 1999; 400:367–371. [PubMed: 10432115]

Foeller E, Celikel T, Feldman DE. Inhibitory sharpening of receptive fields contributes to whisker map plasticity in rat somatosensory cortex. J Neurophysiol. 2005; 94:4387–4400. [PubMed: 16162832]

Fox K. Anatomical pathways and molecular mechanisms for plasticity in the barrel cortex. Neuroscience. 2002; 111:799–814. [PubMed: 12031405]

Froemke RC, Merzenich MM, Schreiner CE. A synaptic memory trace for cortical receptive field plasticity. Nature. 2007; 450:425–429. [PubMed: 18004384]

Fuchs JL, Salazar E. Effects of whisker trimming on GABA(A) receptor binding in the barrel cortex of developing and adult rats. J Comp Neurol. 1998; 395:209–216. [PubMed: 9603373]

Gabernet L, Jadhav SP, Feldman DE, Carandini M, Scanziani M. Somatosensory integration controlled by dynamic thalamocortical feed-forward inhibition. Neuron. 2005; 48:315–327. [PubMed: 16242411]

Galarreta M, Erdelyi F, Szabo G, Hestrin S. Cannabinoid sensitivity and synaptic properties of 2 GABAergic networks in the neocortex. Cereb Cortex. 2008; 18:2296–2305. [PubMed: 18203691]

Gandhi SP, Yanagawa Y, Stryker MP. Delayed plasticity of inhibitory neurons in developing visual cortex. Proc Natl Acad Sci U S A. 2008; 105:16797–16802. [PubMed: 18940923]

Helmstaedter M, Staiger JF, Sakmann B, Feldmeyer D. Efficient recruitment of layer 2/3 interneurons by layer 4 input in single columns of rat somatosensory cortex. J Neurosci. 2008; 28:8273–8284. [PubMed: 18701690]

Holmgren CD, Zilberter Y. Coincident spiking activity induces long-term changes in inhibition of neocortical pyramidal cells. J Neurosci. 2001; 21:8270–8277. [PubMed: 11588198]

Hong EJ, McCord AE, Greenberg ME. A biological function for the neuronal activity-dependent component of Bdnf transcription in the development of cortical inhibition. Neuron. 2008; 60:610–624. [PubMed: 19038219]

Hull C, Isaacson JS, Scanziani M. Postsynaptic mechanisms govern the differential excitation of cortical neurons by thalamic inputs. J Neurosci. 2009; 29:9127–9136. [PubMed: 19605650]

Jadhav SP, Wolfe J, Feldman DE. Sparse temporal coding of elementary tactile features during active whisker sensation. Nat Neurosci. 2009; 12:792–800. [PubMed: 19430473]

Jasinska M, Siucinska E, Cybulska-Klosowicz A, Pyza E, Furness DN, Kossut M, Glazewski S. Rapid, learning-induced inhibitory synaptogenesis in murine barrel field. J Neurosci. 2010; 30:1176–1184. [PubMed: 20089926]

Jiao Y, Zhang C, Yanagawa Y, Sun QQ. Major effects of sensory experiences on the neocortical inhibitory circuits. J Neurosci. 2006; 26:8691–8701. [PubMed: 16928857]

Jiao Y, Zhang Z, Zhang C, Wang X, Sakata K, Lu B, Sun QQ. A key mechanism underlying sensory experience-dependent maturation of neocortical GABAergic circuits in vivo. Proc Natl Acad Sci U S A. 2011; 108:12131–12136. [PubMed: 21730187]

Kameyama K, Sohya K, Ebina T, Fukuda A, Yanagawa Y, Tsumoto T. Difference in binocularity and ocular dominance plasticity between GABAergic and excitatory cortical neurons. J Neurosci. 2010; 30:1551–1559. [PubMed: 20107082]

Kapfer C, Glickfeld LL, Atallah BV, Scanziani M. Supralinear increase of recurrent inhibition during sparse activity in the somatosensory cortex. Nat Neurosci. 2007; 10:743–753. [PubMed: 17515899]

Knott GW, Quairiaux C, Genoud C, Welker E. Formation of dendritic spines with GABAergic synapses induced by whisker stimulation in adult mice. Neuron. 2002; 34:265–273. [PubMed: 11970868]

Kullmann DM, Lamsa KP. Long-term synaptic plasticity in hippocampal interneurons. Nat Rev Neurosci. 2007; 8:687–699. [PubMed: 17704811]

Lin Y, Bloodgood BL, Hauser JL, Lapan AD, Koon AC, Kim TK, Hu LS, Malik AN, Greenberg ME. Activity-dependent regulation of inhibitory synapse development by Npas4. Nature. 2008; 455:1198–1204. [PubMed: 18815592]

Lu JT, Li CY, Zhao JP, Poo MM, Zhang XH. Spike-timing-dependent plasticity of neocortical excitatory synapses on inhibitory interneurons depends on target cell type. J Neurosci. 2007; 27:9711–9720. [PubMed: 17804631]

Lubke J, Roth A, Feldmeyer D, Sakmann B. Morphometric analysis of the columnar innervation domain of neurons connecting layer 4 and layer 2/3 of juvenile rat barrel cortex. Cereb Cortex. 2003; 13:1051–1063. [PubMed: 12967922]

Maffei A, Lambo ME, Turrigiano GG. Critical period for inhibitory plasticity in rodent binocular V1. J Neurosci. 2010; 30:3304–3309. [PubMed: 20203190]

Maffei A, Nataraj K, Nelson SB, Turrigiano GG. Potentiation of cortical inhibition by visual deprivation. Nature. 2006; 443:81–84. [PubMed: 16929304]

Maffei A, Nelson SB, Turrigiano GG. Selective reconfiguration of layer 4 visual cortical circuitry by visual deprivation. Nat Neurosci. 2004; 7:1353–1359. [PubMed: 15543139]

Maffei A, Turrigiano GG. Multiple modes of network homeostasis in visual cortical layer 2/3. J Neurosci. 2008; 28:4377–4384. [PubMed: 18434516]

Marik SA, Yamahachi H, McManus JN, Szabo G, Gilbert CD. Axonal dynamics of excitatory and inhibitory neurons in somatosensory cortex. PLoS Biol. 2010; 8:e1000395. [PubMed: 20563307]

Micheva KD, Beaulieu C. An anatomical substrate for experience-dependent plasticity of the rat barrel field cortex. Proc Natl Acad Sci U S A. 1995; 92:11834–11838. [PubMed: 8524859]

Miller KD, Pinto DJ, Simons DJ. Processing in layer 4 of the neocortical circuit: new insights from visual and somatosensory cortex. Curr Opin Neurobiol. 2001; 11:488–497. [PubMed: 11502397]

Mrsic-Flogel TD, Hofer SB, Ohki K, Reid RC, Bonhoeffer T, Hubener M. Homeostatic regulation of eye-specific responses in visual cortex during ocular dominance plasticity. Neuron. 2007; 54:961–972. [PubMed: 17582335]

Poleg-Polsky A, Diamond JS. Imperfect Space Clamp Permits Electrotonic Interactions between Inhibitory and Excitatory Synaptic Conductances, Distorting Voltage Clamp Recordings. PLoS One. 2011; 6:e19463. [PubMed: 21559357]

Pouille F, Marin-Burgin A, Adesnik H, Atallah BV, Scanziani M. Input normalization by global feedforward inhibition expands cortical dynamic range. Nat Neurosci. 2009; 12:1577–1585. [PubMed: 19881502]

Pouille F, Scanziani M. Enforcement of temporal fidelity in pyramidal cells by somatic feed-forward inhibition. Science. 2001; 293:1159–1163. [PubMed: 11498596]

Priebe NJ, Ferster D. Inhibition, spike threshold, and stimulus selectivity in primary visual cortex. Neuron. 2008; 57:482–497. [PubMed: 18304479]

Reyes A, Lujan R, Rozov A, Burnashev N, Somogyi P, Sakmann B. Target-cell-specific facilitation and depression in neocortical circuits. Nat Neurosci. 1998; 1:279–285. [PubMed: 10195160]

Rubenstein JL, Merzenich MM. Model of autism: increased ratio of excitation/inhibition in key neural systems. Genes Brain Behav. 2003; 2:255–267. [PubMed: 14606691]

Shepherd GM, Pologruto TA, Svoboda K. Circuit analysis of experience-dependent plasticity in the developing rat barrel cortex. Neuron. 2003; 38:277–289. [PubMed: 12718861]

Stern EA, Maravall M, Svoboda K. Rapid development and plasticity of layer 2/3 maps in rat barrel cortex in vivo. Neuron. 2001; 31:305–315. [PubMed: 11502260]

Sun QQ. Experience-dependent intrinsic plasticity in interneurons of barrel cortex layer IV. J Neurophysiol. 2009; 102:2955–2973. [PubMed: 19741102]

Swadlow HA. Thalamocortical control of feed-forward inhibition in awake somatosensory 'barrel' cortex. Philos Trans R Soc Lond B Biol Sci. 2002; 357:1717–1727. [PubMed: 12626006]

Traub RD, Buhl EH, Gloveli T, Whittington MA. Fast rhythmic bursting can be induced in layer 2/3 cortical neurons by enhancing persistent Na+ conductance or by blocking BK channels. J Neurophysiol. 2003; 89:909–921. [PubMed: 12574468]

Turrigiano GG, Nelson SB. Hebb and homeostasis in neuronal plasticity. Curr Opin Neurobiol. 2000; 10:358–364. [PubMed: 10851171]

Turrigiano GG, Nelson SB. Homeostatic plasticity in the developing nervous system. Nat Rev Neurosci. 2004; 5:97–107. [PubMed: 14735113]

Wehr M, Zador AM. Balanced inhibition underlies tuning and sharpens spike timing in auditory cortex. Nature. 2003; 426:442–446. [PubMed: 14647382]

Wigstrom H, Gustafsson B. Postsynaptic control of hippocampal long-term potentiation. J Physiol (Paris). 1986; 81:228–236. [PubMed: 2883309]

Wilent WB, Contreras D. Dynamics of excitation and inhibition underlying stimulus selectivity in rat somatosensory cortex. Nat Neurosci. 2005; 8:1364–1370. [PubMed: 16158064]

Williams SR, Mitchell SJ. Direct measurement of somatic voltage clamp errors in central neurons. Nat Neurosci. 2008; 11:790–798. [PubMed: 18552844]

Yazaki-Sugiyama Y, Kang S, Cateau H, Fukai T, Hensch TK. Bidirectional plasticity in fast-spiking GABA circuits by visual experience. Nature. 2009; 462:218–221. [PubMed: 19907494]

Highlights

- Whisker deprivation reduces feedforward inhibition during whisker map plasticity
- Feedforward inhibition is reduced in parallel with feedforward excitation
- Reduced inhibition maintains excitation-inhibition balance during plasticity
- Multiple sites of plasticity exist within fast-spiking (FS) interneuron circuits

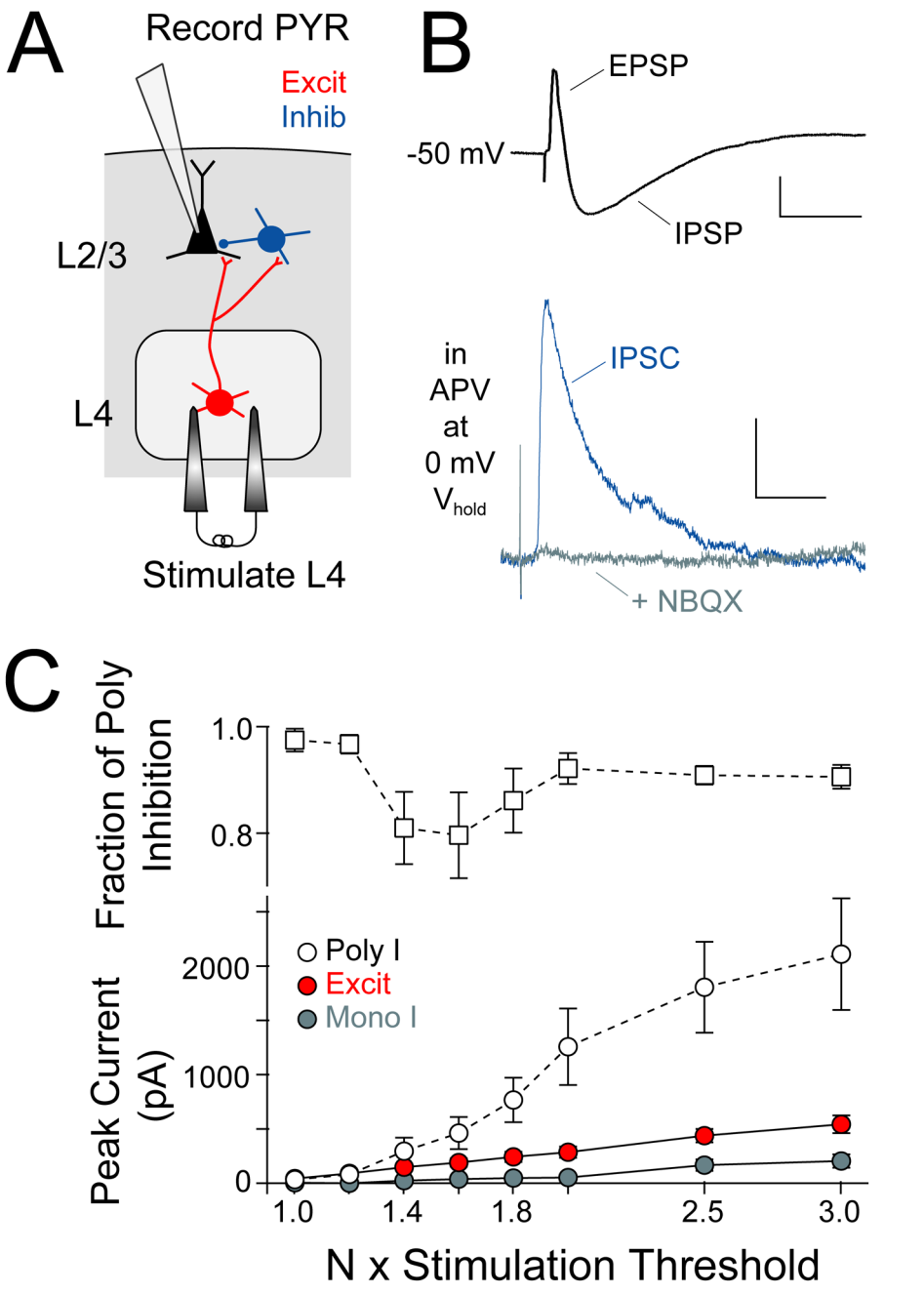

Figure 1. Measurement of L4-evoked feedforward inhibition in L2/3 pyramidal cells

(**A**) Experimental design for recording L4-evoked excitatory and inhibitory responses. **(B)** Top, Example L4-evoked EPSP-IPSP sequence (scale bar: 2 mV, 50 ms). Bottom, L4-evoked IPSC at 0 mV before and after NBQX, which blocks polysynaptic inhibition (scale bar: 50 pA, 20 ms). (**C**) Mean input-output curves showing recruitment of IPSCs and EPSCs with increasing L4 stimulation intensity. Mono- and polysynaptic inhibition were separated using NBQX. Top, Fraction of inhibition that was polysynaptic at each stimulation intensity. In this and all figures, data represent mean ± SEM unless otherwise noted.

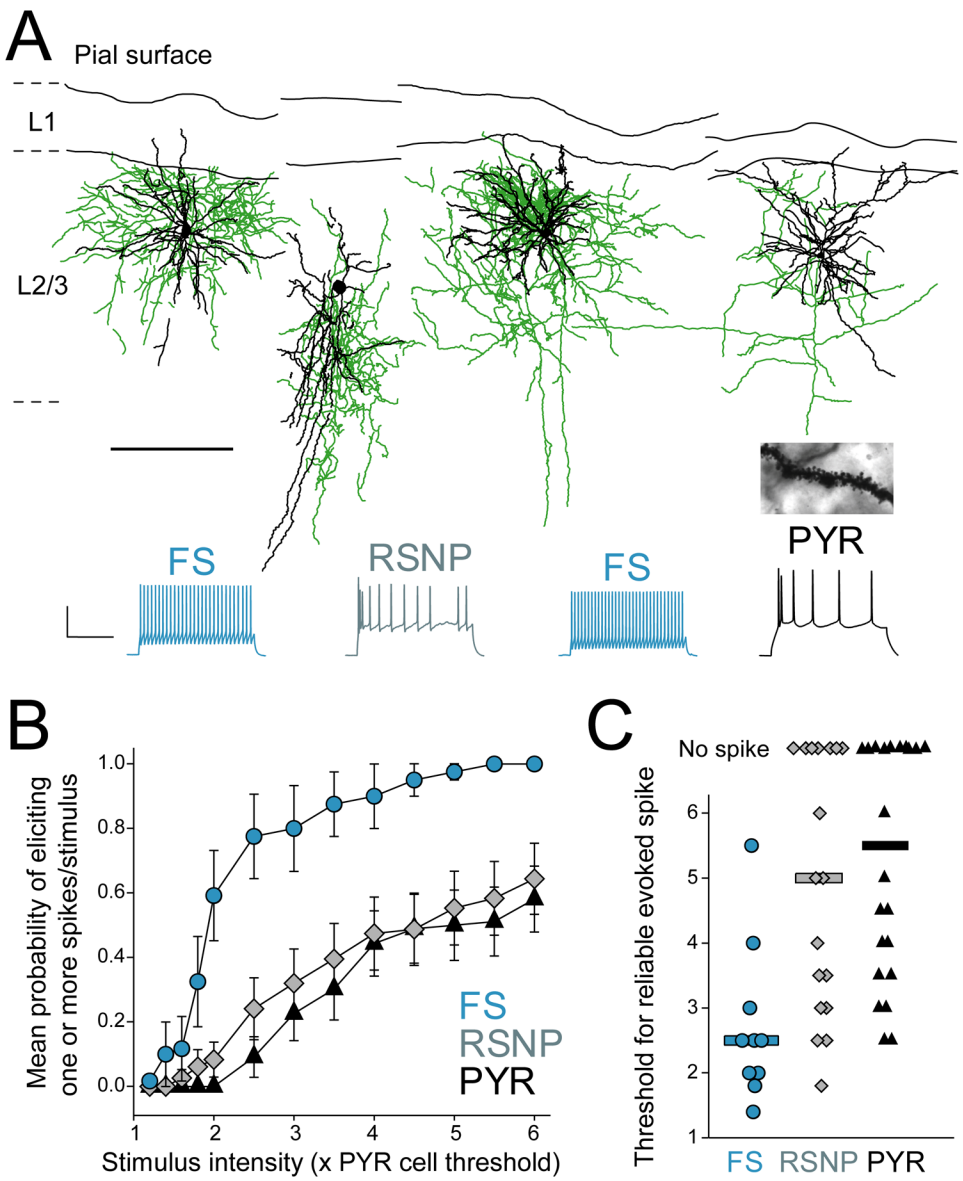

Figure 2. FS cells mediate L4-evoked feedforward inhibition in L2/3

(**A**) Example biocytin reconstructions of physiologically identified FS basket, RSNP and PYR cells. Axons are green and dendrites are black (scale bar: 200 μm). Inset, spiny dendrites of putative PYR cell. Below, spike patterns from each cell (scale bar: 40 mV, 200 ms). (**B**) L4-evoked firing probability of FS cells, RSNP cells and PYR cells. (**C**) Threshold L4 stimulation intensity to evoke ≥ 1 spike/stimulus in each cell. Bars are median. See also Figure S1.

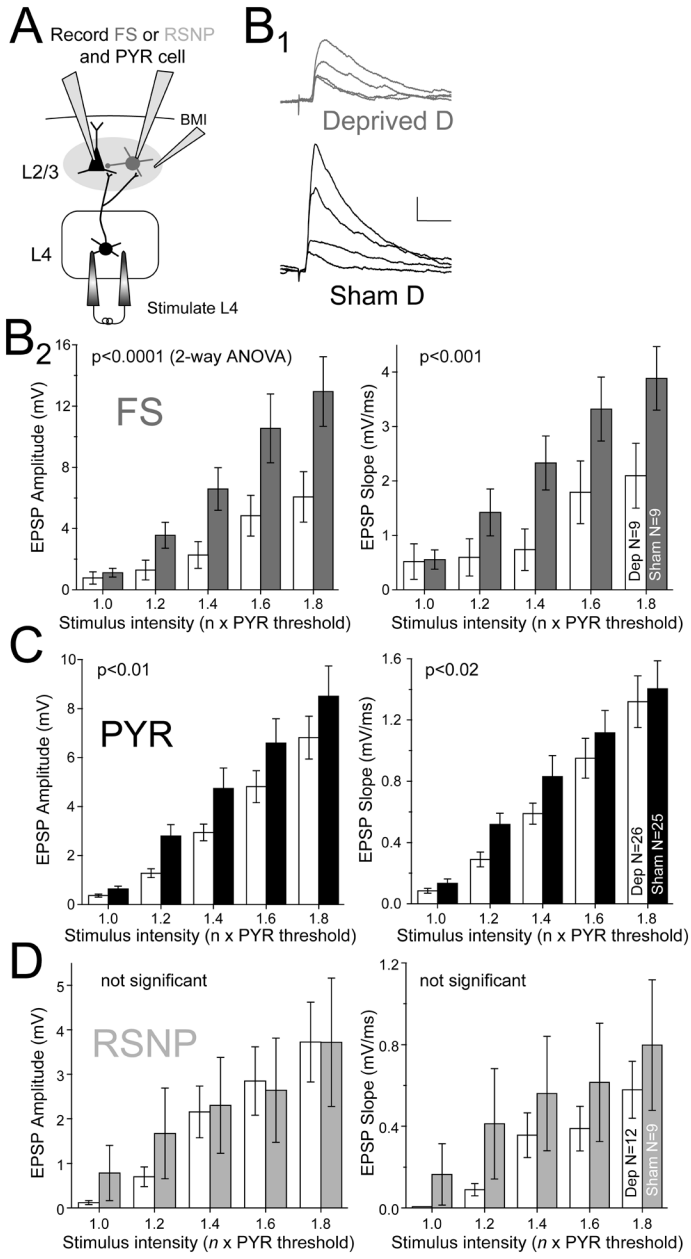

Figure 3. Deprivation weakens L4 to L2/3 excitation onto FS and pyramidal cells

(**A**) Experimental design for recording L4 excitation onto L2/3 FS, RSNP, and PYR cells. Bicuculline methiodide (BMI) was applied focally. (**B1**) L4-evoked EPSPs in two representative FS cells (stimulation intensities: 1.0, 1.2, 1.4, and 1.6 x excitatory response threshold for a co-columnar PYR cell). Scale bar: 1 mV, 20 ms. (**B2**) Mean input-output curves for L4-evoked EPSPs onto L2/3 FS cells. Significance between deprived and spared columns is shown (ANOVA). (**C** and **D**) Mean input-output curves for EPSP amplitude and slope for L2/3 PYR cells (**C**) and RSNP cells (**D**). Bars are mean ± SEM.

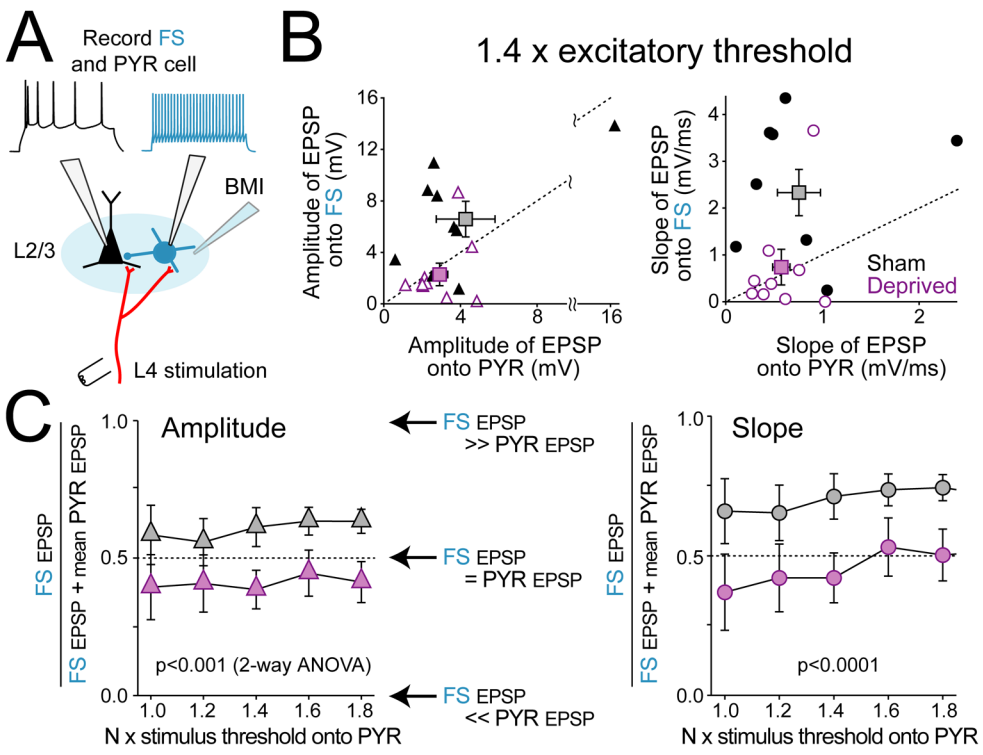

Figure 4. Deprivation weakens excitation onto FS cells more than onto PYR cells

(**A**) Experiment design. (**B**) Comparison of L4-evoked EPSPs onto co-columnar FS and PYR cells (measured at 1.4 x excitatory response threshold). Each symbol is one FS-PYR cell pair. Squares show mean ± SEM. Diagonal shows equality. (**C**) Relative excitation onto FS vs. PYR cells, quantified as (FS EPSP/(FS EPSP + mean pyramidal EPSP)), for each L4 stimulation intensity. Left, quantification for EPSP amplitude. Right, for EPSP slope. Dashed line indicates equal EPSPs onto FS and PYR cells. When more than one PYR cell was recorded in a single column, the mean EPSP value was used.

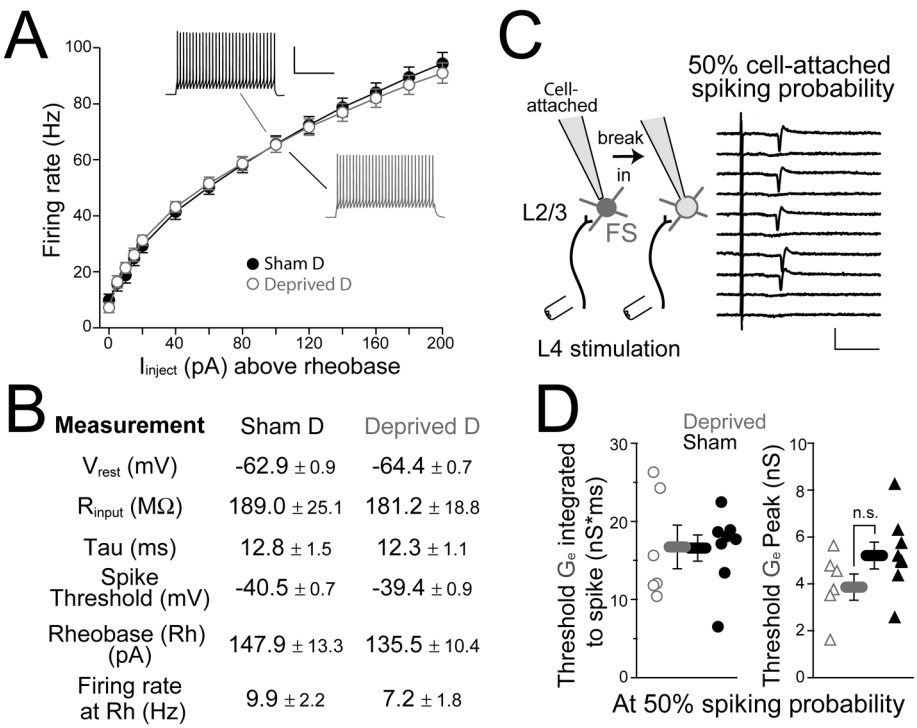

Figure 5. Intrinsic and synaptically driven excitability of FS cells are unaltered by deprivation

(**A**) Current-firing rate relationship for FS cells, for 500-ms current injection. Rheobase is the current required to elicit a single spike. Scale bar: 40 mV, 200 ms. (**B**) Intrinsic properties of FS cells in deprived vs. sham-deprived D columns. Tau is the membrane time constant. (**C**) Left, experimental design to measure the L4-evoked excitatory conductance required to elicit 50% spike probability in an FS cell. Right, consecutive sweeps showing L4-evoked spikes recorded in cell-attached mode from an FS cell at 50% spike probability. Scale bar: 50 pA, 10 ms. (**D**) Peak and integrated G_e at 50% spike probability (integrated from response onset to spike latency for each neuron) for cells from deprived vs. sham-deprived rats. See also Figure S2.

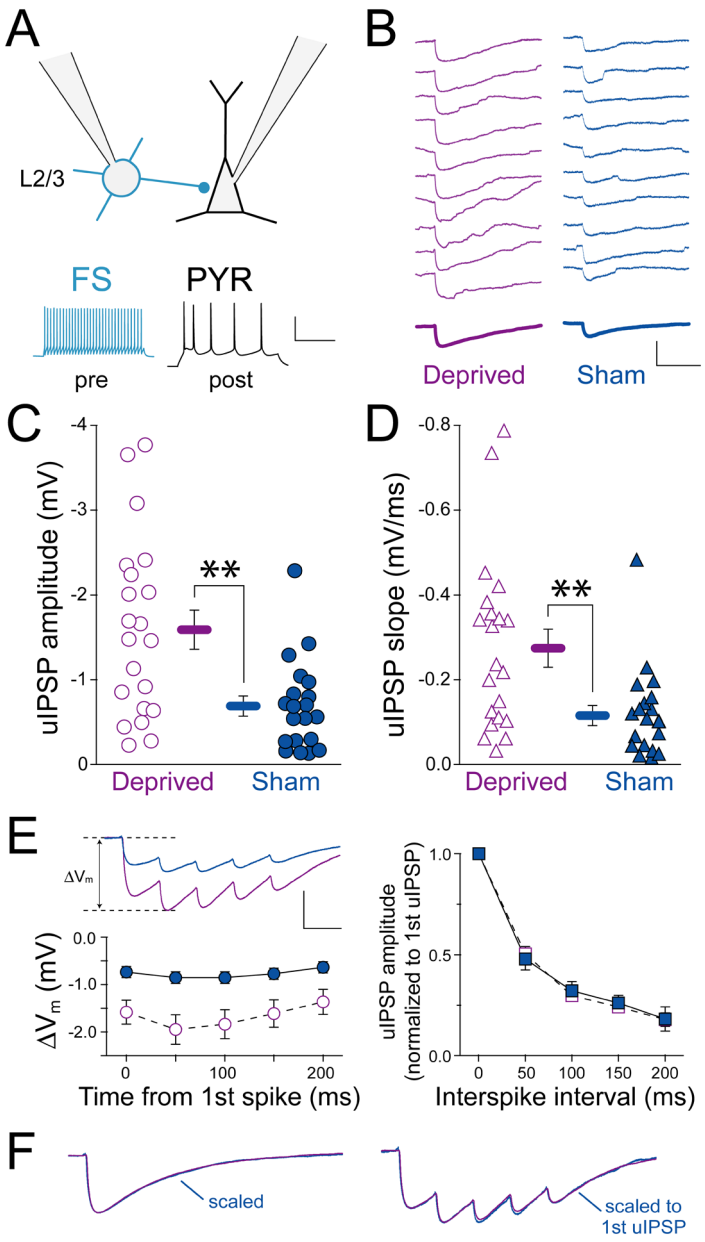

Figure 6. Deprivation potentiates L2/3 FS→PYR unitary IPSPs

(**A**) Experimental design with example pre- and postsynaptic spike patterns. Scale bar: 50 mV, 200 ms. (**B**) Consecutive single-sweep uIPSPs from a deprived and a sham-deprived L2/3 FS→PYR pair. Bold, average uIPSP. Scale bar: 2.5 mV, 100 ms. (**C, D**) Mean uIPSP amplitude and slope for each connected pair. Bars are mean ± SEM; **, $p < 0.01$. (**E**) Responses to trains of 5 FS spikes (50 ms interval). Top, average uIPSP train for 20 deprived FS→PYR pairs and 19 sham-deprived pairs. Bottom left, mean ΔV_m for each uIPSP in the train. Scale bar: 1 mV, 50 ms. Right, amplitude of each uIPSP normalized to first uIPSP amplitude, showing no difference in short-term plasticity between deprived and sham-deprived pairs. (**F**) Left, mean single-spike uIPSP for all cells in deprived and sham-deprived columns, peak normalized to show IPSP decay kinetics. Right, mean response to 5-spike train, normalized to the first uIPSP peak (same scale bar as in E).

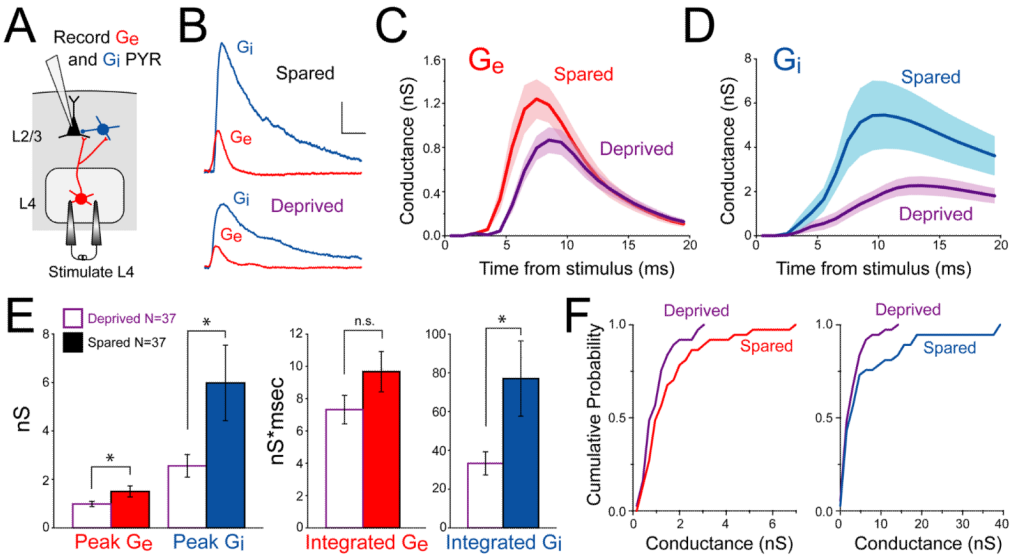

Figure 7. Whisker deprivation reduces L4-evoked excitation and inhibition onto L2/3 pyramidal cells

(**A**) Experimental design. (**B**) Example G_e and G_i measured in two L2/3 pyramidal cells. Scale bar: 1 nS, 10 ms. (**C** and **D**) Average G_e and G_i waveforms for neurons in spared vs. deprived columns. 1 ms bins. Shading shows SEM. (**E**) Peak (left) and integrated (right) G_e and G_i in spared vs. deprived columns; *, $p < 0.05$. (**F**) Cumulative distribution of peak data from (**E**). See also Figure S3 and S4.

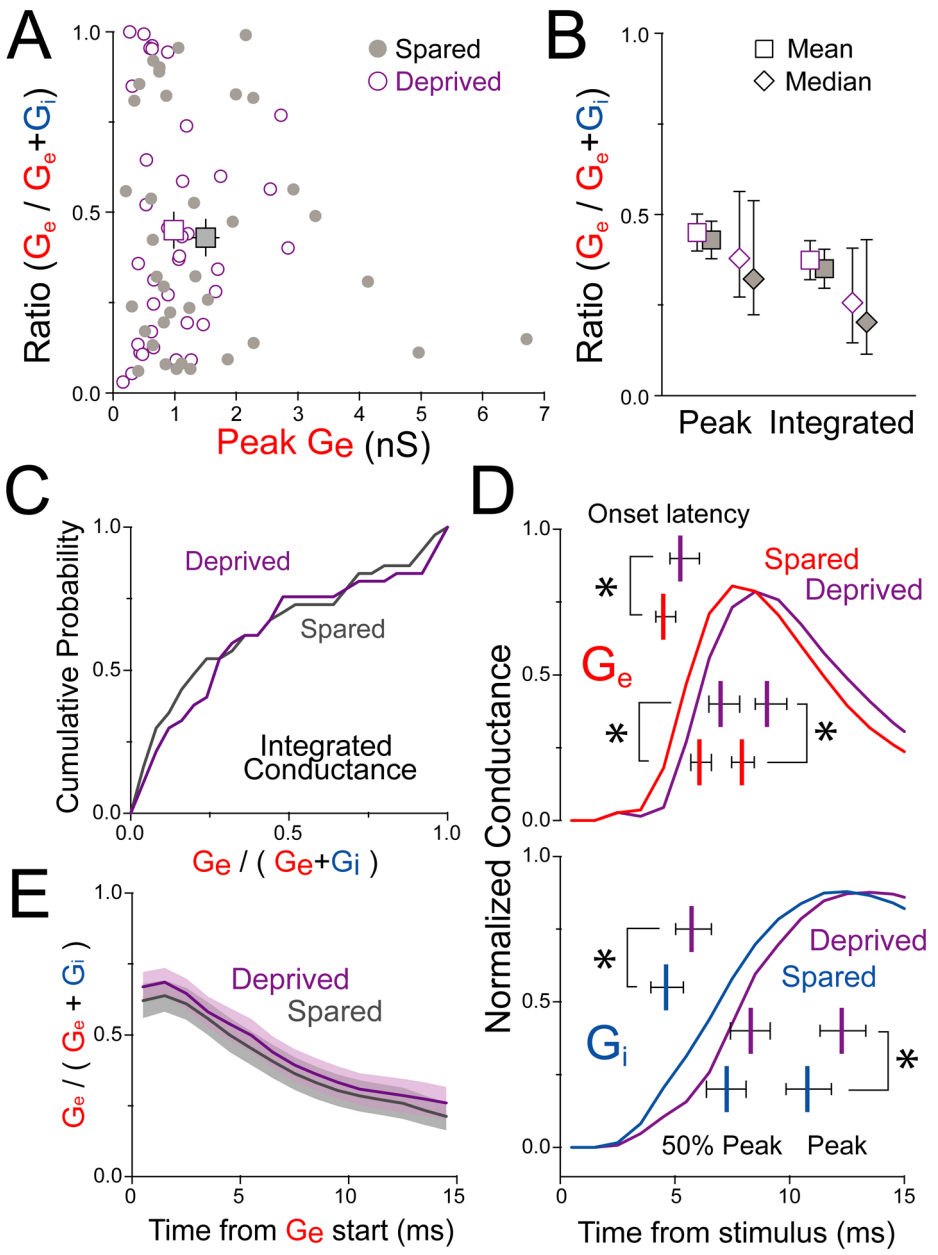

Figure 8. Deprivation preserves the balance and relative timing of excitation and inhibition

(**A**) G_e fraction is broadly distributed and not altered by deprivation. (**B**) Mean ± SEM and median ± 95 % confidence intervals for G_e fraction calculated from peak or integrated G_e and G_i. (**C**) Cumulative distribution of G_e fraction based on integrated conductance. (**D**) Mean peak-normalized G_e and G_i recorded in spared B vs. deprived D columns. Bars, mean ± 95% confidence intervals for G_e and G_i onset latency, latency to 50% of peak and peak latency. *, $p < 0.05$, ranksum test. (**E**) G_e fractional conductance over the first 15 ms from G_e start. See also Table S1 and Figure S5.